Dynamic Modeling of Adjustable-Speed Pumped Storage Hydropower Plant

Preprint

E. Muljadi, M. Singh, and V. Gevorgian
National Renewable Energy Laboratory

M. Mohanpurkar and R. Hovsapian
Idaho National Laboratory

V. Koritarov
Argonne National Laboratory

To be presented at the 2015 IEEE Power and Energy Society General Meeting
Denver, Colorado
July 26–30, 2015

NREL is a national laboratory of the U.S. Department of Energy
Office of Energy Efficiency & Renewable Energy
Operated by the Alliance for Sustainable Energy, LLC

This report is available at no cost from the National Renewable Energy Laboratory (NREL) at www.nrel.gov/publications.

Conference Paper
NREL/CP-5D00-63587
April 2015

Contract No. DE-AC36-08GO28308

This report is available at no cost from the National Renewable Energy Laboratory (NREL) at www.nrel.gov/publications.

Available electronically at http://www.osti.gov/scitech

Available for a processing fee to U.S. Department of Energy and its contractors, in paper, from:

U.S. Department of Energy
Office of Scientific and Technical Information
P.O. Box 62
Oak Ridge, TN 37831-0062
phone: 865.576.8401
fax: 865.576.5728
email: mailto:reports@adonis.osti.gov

Available for sale to the public, in paper, from:

U.S. Department of Commerce
National Technical Information Service
5285 Port Royal Road
Springfield, VA 22161
phone: 800.553.6847
fax: 703.605.6900
email: orders@ntis.fedworld.gov
online ordering: http://www.ntis.gov/help/ordermethods.aspx

Cover Photos: (left to right) photo by Pat Corkery, NREL 16416, photo from SunEdison, NREL 17423, photo by Pat Corkery, NREL 16560, photo by Dennis Schroeder, NREL 17613, photo by Dean Armstrong, NREL 17436, photo by Pat Corkery, NREL 17721.

NREL prints on paper that contains recycled content.

Dynamic Modeling of Adjustable-Speed Pumped Storage Hydropower Plant

E. Muljadi, *Fellow, IEEE*, M. Singh, *Member, IEEE*, V. Gevorgian, *Member, IEEE*, M. Mohanpurkar, *Member, IEEE*, R. Hovsapian, *Senior Member, IEEE*, and V. Koritarov, *Member, IEEE*

***Abstract*--Hydropower is the largest producer of renewable energy in the U.S. More than 60% of the total renewable generation comes from hydropower. There is also approximately 22 GW of pumped storage hydropower (PSH). Conventional PSH uses a synchronous generator, and thus the rotational speed is constant at synchronous speed.**

This work details a hydrodynamic model and generator/power converter dynamic model. The optimization of the hydrodynamic model is executed by the hydro-turbine controller, and the electrical output real/reactive power is controlled by the power converter. All essential controllers to perform grid-interface functions and provide ancillary services are included in the model.

***Index Terms*--hydropower plant, energy storage, pumped storage hydropower, adjustable speed, variable speed, ancillary services, frequency response**

I. Introduction

The U.S. Department of Energy Water Power Program has a goal of hydropower providing 15% of our nation's electricity by 2030. A hydropower plant is a mature technology; in fact, it is one of the oldest commonly used sources of energy. It is used to supply energy needs in many nations. The largest hydropower plant, Three Gorges in Hubei Province, China, generates 22.4 GW of power. The second largest hydropower plant is Itaipu, located in Brazil, which has an installed capacity of 14 GW. Next are Xiluodu, in China, at 13.8 GW; and Simón Bolívar, in Venezuela, which has an installed capacity of 10.2 GW.

In the U.S., the expansion of hydropower plants could potentially make a significant positive impact, because hydropower is the largest producer of renewable energy. More than 60% of the total renewable generation in the U.S. comes from hydropower plants. A hydroelectric power plant converts the potential energy of water flowing from a higher elevation through a penstock to a lower elevation where a water turbine is used to drive an electric generator. The size of the potential energy of the water is determined by the amount of water and the head (the height from the base to the water surface of the reservoir).

Conventional pumped storage hydropower (PSH) uses a synchronous generator, and hence its rotational speed is constant at synchronous speed. Control of output power in such plants is based on the adjustment of the wicket gates to increase or decrease water flow, and thus the response time of a conventional PSH plant necessary to change the electrical output power is determined by the mechanical time constant to operate the wicket gates controller.

In Europe, many PSH plants are planned to be installed between 2011 and 2020. Out of the total 11,562 MW PSH to be installed, 59% is conventional PSH, 3% is ternary PSH, and 38% is adjustable-speed PSH (AS-PSH) [1]. One of the older references on AS-PSH can be found in an IEEE paper from 1980 [2]. Ref. [3] provides a good informational background on the basic concept of AS-PSH. References [4-7] document the AS-PSH studies and implementations in Europe, North America, and Japan.

In this paper, the foundation of the AS-PSH including the control of the generator and power converter is presented in Section III. The simulation results are discussed in Section IV, which is followed by a conclusion in Section V.

II. AH-PSH

AS-PSH is an extension of conventional PSH in which the synchronous generator is replaced by a doubly-fed induction generator (DFIG). A DFIG connected to a hydro turbine resembling an AS-PSH is shown in Fig. 1.

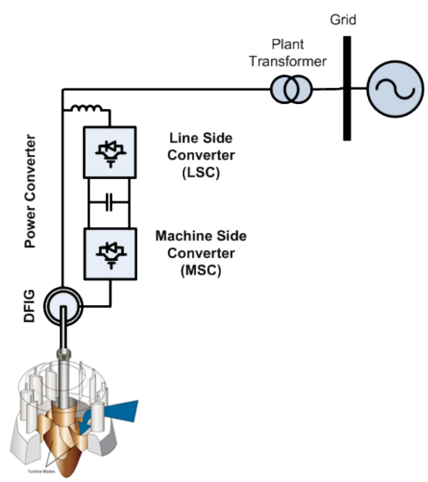

Fig. 1. Diagram of the physical connection of a DFIG in an AS-PSH. Inset: Image from Wikipedia [8]

In the design of a PSH system, transient effects are an important consideration. Such transient effects can originate from both hydrodynamic and electromagnetic phenomena. It is well known that rapid flow variations can lead to potentially catastrophic increases in pressure.

Numerical techniques for hydraulic transient analysis appear to be well understood but still need some improvements for adjustable-speed reversible pump-turbine applications.

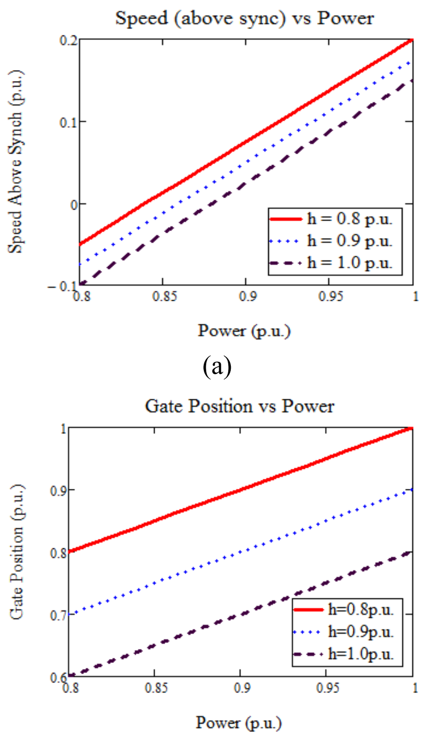

(a) (b)

Fig. 2. Optimum operation of AS-PSH at different power levels as a function of the head (a) rotor speed and (b) gate position.

AS-PSH is normally optimized to maximize the efficiency of the hydro turbine. The typical optimum operation of a hydro turbine can be found in [9]. Fortunately, for each different head there is a linear relationship between the rotational speed and the output power of the hydro turbine, as shown in Fig. 2(a), and it can be written as

$$\omega_m\left(head, P_{ref}\right) = -0.05 + 1.25\left(P_{ref} - 0.8\right) - 0.25(head - 0.8) \quad (1)$$

Similarly, for different head levels there is a linear relationship between the wicket gate positions (to adjust the water flow) as the output power is changed from one value to another, as shown in Fig. 2(b), which can be described by

$$Gate\left(head, P_{ref}\right) = 0.8 + \left(P_{ref} - 0.8\right) - (head - 0.8) \quad (2)$$

The water level typically varies very slowly, especially when the size of the reservoir and/or the incoming water flow is sufficiently large. However, to optimize the turbine operation, it is necessary to adjust the gate position and the rotational speed as the head varies with time. This type of adjustment can be done via software and preprogrammed look-up table for acceptable optimal values at a particular AS-PSH station.

A. DFIG with a Partial Rating Power Converter

Since it was invented by Nikola Tesla in 1883, this electric machine has been preferred for extensive industrial applications because of its numerous advantages. One such advantage is that induction machines allow for variable-speed operation with a relatively simple design modification—i.e., inserting a variable rotor resistance into the rotor winding via a three-phase slip ring. Recently, the use of wound-rotor induction machines has been revived in the form of induction generators for wind turbine applications. With the power converter connected to the rotor winding, the induction generator can be operated at variable speed using a partial-rating power converter. Reference [10] presents various generator converter technologies, including DFIG.

1) Basic Equations

From the equivalent circuit of a DFIG, which is shown in Fig. 3, we can derive the equations to determine the size of power converter needed.

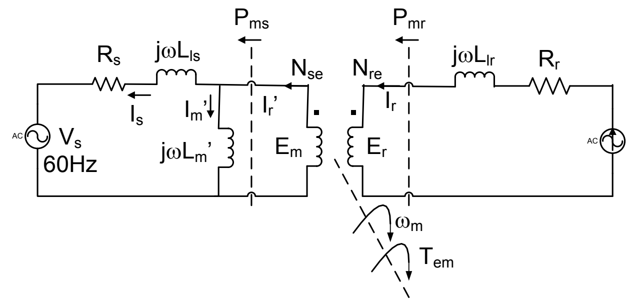

Fig. 3. Per-phase equivalent circuit of the induction generator.

From the equivalent circuit, the induced rotor emf E_r is proportional to the winding ratio and to the rotor frequency. In a locked rotor condition (slip=1), the stator-to-rotor winding relationship is similar to a transformer. As the slip gets smaller, the rotor voltage decreases. The relationship between the stator emf E_s and slip can be written as

$$\frac{\boldsymbol{E_{mr}}}{\boldsymbol{E_{ms}}} = \boldsymbol{s}\,\frac{\boldsymbol{N_{re}}}{\boldsymbol{N_{se}}}\,\langle\,\boldsymbol{\theta_e} \quad (3)$$

The current ratio is not affected by the rotor frequency and can be written as

$$\frac{\boldsymbol{I_r}}{\boldsymbol{I_s}} = \frac{N_{se}}{N_{re}}\,\langle\,\theta_e \quad (4)$$

The ratio of the actual rotor impedance to the stator referred rotor impedance is given by

$$\frac{\boldsymbol{Z_r}}{\boldsymbol{Z_r}'} = \boldsymbol{s}\left[\frac{N_{re}}{N_{se}}\right]^{2} \quad (5)$$

The useful active power at the stator side can be computed as

$$P_{ms} = Re[\boldsymbol{I_{ms}}\boldsymbol{E_{ms}}^{*}] \quad (6)$$

The real power at the rotor side can be computed as

$$P_{mr} = Re[\boldsymbol{I_{mr}}\boldsymbol{E_{mr}}^{*}] \quad (7)$$

By substitution, we get

$$P_{mr} = Re[s\,\boldsymbol{I_{ms}}\boldsymbol{E_{ms}}^{*}] \quad (8)$$

Or

$$P_{mr} = s\,P_{ms} \quad (9)$$

Of the total air gap power of the generator, only a small fraction is dissipated in the rotor circuits. The total electrical output power generated to the grid is given by

$$P_{total} = (P_{ms} - P_{mr}) = (1 - s)P_{ms} \quad (10)$$

Thus, total power generated by the hydro turbine is converted into electrical power delivered to the grid, the majority via the stator winding and the rest via the rotor output power. For example, assuming the turns ratio of the stator-to-rotor winding is one, the DFIG needs to be operated at $\pm$ 30% slip. The power converter to be used must have a rated voltage of approximately 30% and rated current of 100%. The implication is that using a DFIG in variable speed with slip variation from -30% to +30% requires the size of the power converter to be approximately 30% of the rated power of the induction generator.

B. Control Algorithm

This section presents the control algorithms for both the hydro turbine and the DFIG.

1) Hydro Turbine Control

The hydro turbine control is based on optimization of the hydro turbine operation, as discussed in the previous section. The optimum operation of the hydro turbine is determined by the rotational speed and the gate position, as shown in equations (1-2). The two variables (speed, gate) are computed for every commanded output power (P_{ref}). The following block diagrams can be used to illustrate the algorithm for hydro turbine control.

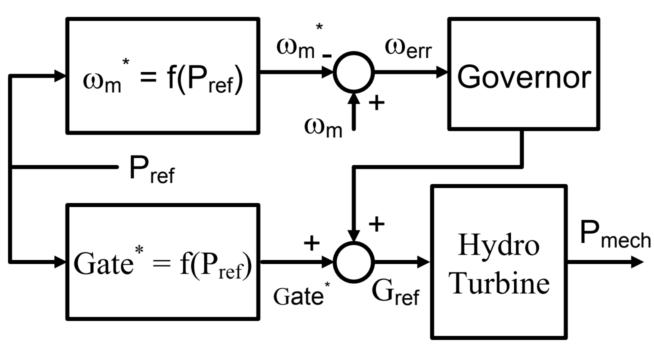

Fig. 4. Simplified diagram of hydro turbine control.

2) Power Converter and Generator Control

The power converter and the DFIG are controlled based on the equations derived in the previous section. The reference power is the commanded power output of the hydro turbine. The DFIG has two separate paths of generation: the stator output power and the rotor output power. The output power from the stator winding (always flowing out of the stator to the grid) can be described as

$$P_{ms} = \frac{P_{total}}{(\mathbf{1} - \boldsymbol{s})} \quad (11)$$

Stator power generated by the DFIG as a function of the total power is illustrated in Fig. 5. As shown, the variation of the stator power is very narrow. For example, in the span of 0.2 p.u. total power variation, the stator power varies by approximately 2%.

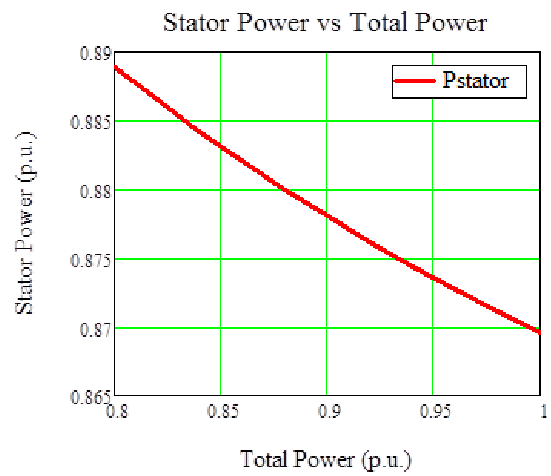

Fig. 5. Stator power as a function of total power.

The rotor power can be computed as

$$P_{mr} = \frac{s}{(\mathbf{1} - \boldsymbol{s})} P_{total} \quad (12)$$

Thus, the total power entering the rotor winding of the DFIG is as shown in Fig. 6.

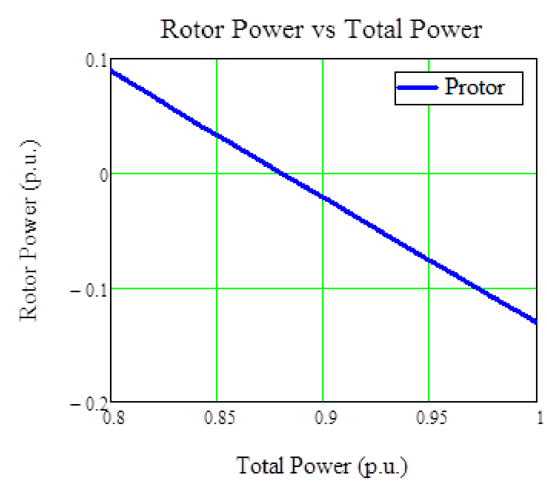

Fig. 6. Rotor power as a function of total power.

As shown, the variation of the rotor power is linear to the total power variation. For example, in the span of 0.2 p.u. total power variations, the rotor power varies by approximately +/- 12%. Note that the rotor power becomes zero at the synchronous speed (slip=0). Below the synchronous speed, the rotor power flows from the grid into the rotor winding; and above synchronous speed, the rotor power flows from the rotor winding to the grid.

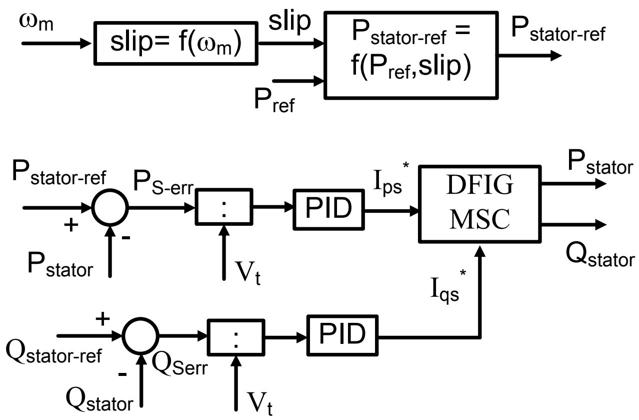

Fig. 7. Simplified diagram of MSC .

As shown in Fig. 7, the machine-side converter (MSC) is used to control the commanded stator output power (Pstator-ref) based on the calculated reference that will optimize the hydro turbine. And the reactive power is controlled to follow the commanded reactive power output of the stator winding (Qstator-ref). The real power component of the stator current IpS and the reactive power component of the stator current IqS are controlled by the MSC.

As shown in Fig. 8, the line-side converter (LSC) is controlled to maintain the DC bus constant and the reactive power contribution from the LSC to the grid. Note that by controlling the DC bus constant, the LSC automatically transfers the rotor power to the grid. The real power component of the current IpLSC is controlled to maintain the DC bus voltage, whereas the reactive power component of the current IqLSC is used to control the requested reactive power from the LSC.

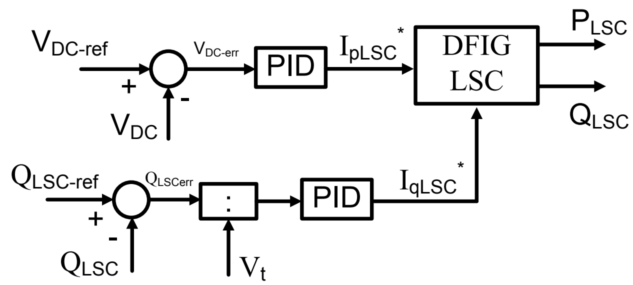

Fig. 8. Simplified diagram of LSC.

III. Dynamic Simulation

To study the interaction between the AS-PSH and the grid, a simple three-generator system is used to understand the dynamic behavior of AS-PSH. The cases we simulated are based on previous work for dynamic model validation performed on the PSS/E platform as found in Ref. [11]. The PSCAD dynamic model we developed is based on the three-phase domain, and it can be used to simulate an unbalanced system.

A. Power System Network

The case under consideration is shown in Fig. 9. It is a simple three-bus system with a very large AS-PSH connected to 1.3 MW loads and two other generators.

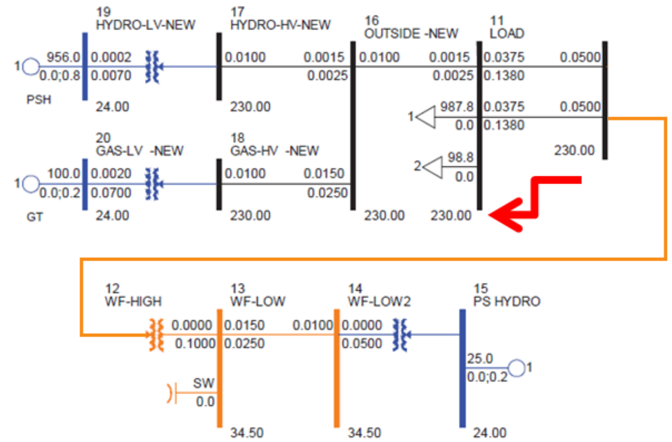

Fig. 9. Single-line diagram of the power system network.

B. Case Study—Line Faults

In the power system network the AS-PSH is connected to Bus 19 at 24 kV. It generates energy to supply the majority of the loads (1.1 MW). The fault is applied to the load bus (Bus 11) at 230 kV. The second generator, 100 MW, is connected to Bus 20 at 24 kV; and the third generator, 25 MW, is connected to Bus 15.

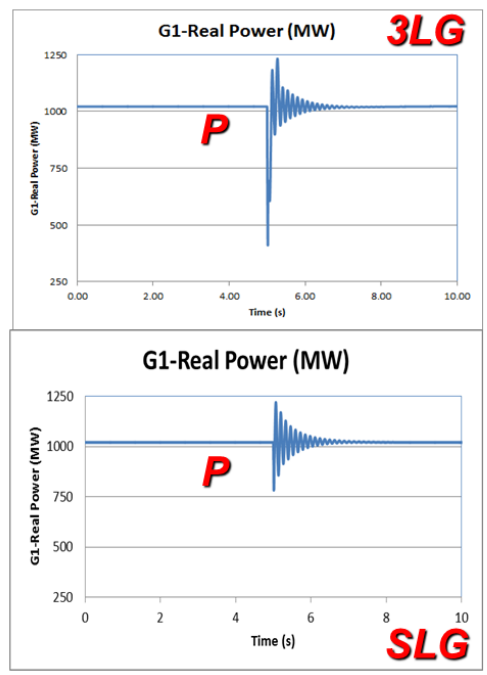

Fig. 10. Real power comparison of 3LG to SLG.

The simulation is conducted for two different faults at 15 milliseconds duration for a) three lines to ground (3LG) and b) single line to ground (SLG). The responses are observed at the output of the AS-PSH at Bus 19. Both the real power and reactive power are recorded and compared. As shown in Fig. 10 and Fig. 11, respectively, the system recovers to steady state in the post-fault recovery region. It is shown that both real and reactive power drop very significantly for the 3LG fault compared to the SLG fault. Note that the AS-PSH under discussion is set to maintain the voltage (Q-priority) during the fault.

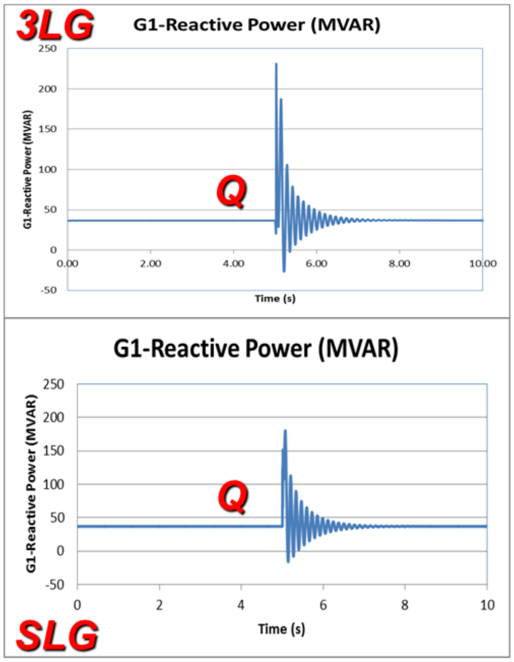

Fig. 11. Reactive power comparison of 3LG to SLG.

The real power fluctuations indicate the behavior of the electromechanical interactions within AS-PSH (including the strains and stresses) and between AS-PSH and the grid. The reactive power fluctuations indicate the voltage control interactions between the AS-PSH and the grid.

IV. Conclusions

This paper is based on the dynamic modeling of AS-PSH. The details of the dynamic modeling of both the hydrodynamic model and the generator-power converter model are not described in this paper because of space limitations. In the power converter and the generator, the frequency response, fault ride-through, and voltage/reactive power controls are included in the actual model. Similarly, the detailed hydrodynamic dynamic equations are included in the actual implementation.

A combined operational control methodology for a hydro turbine and DFIG is presented and implemented in this study as an integrated control topology. In the AS-PSH system, the water resource is generally predictable and available when needed, and thus the power command P_{ref} can be scheduled relatively easily, which provides a dispatchable renewable resource. The optimization is executed via the speed control of the hydro turbine based on the power command P_{ref} and the head. The power converter also takes the P_{ref} as the power command, but it includes an additional power command to perform ancillary services when needed (inertial/frequency response, etc.). The reactive power control is implemented via the power converter control.

Overall, the implementation of the AS-PSH has been very successful, and the model has proven to be very stable in operation. Additional simulation cases were performed but not included in this paper because of space limitations.

V. Acknowledgment

This work was supported by the U.S. Department of Energy under Contract No. DE-AC36-08-GO28308 with the National Renewable Energy Laboratory. This work is collaboration among the National Renewable Energy Laboratory, Idaho National Laboratory, and Argonne National Laboratory.

VI. References

[1] T. Key, “Quantifying the Value of Hydropower in the Electric Grid,” Electric Power Research Institute, Palo Alto, CA, Tech. Rep. 1023144, Feb. 2013.

[2] R. J. Kerkman, T. A. Lipo, W. G. Newman, J. E. Thirkell, “An inquiry into adjustable speed operation of a pumped hydro plant,” *IEEE Trans. Power App. Syst.*, vol. PAS-99, no. 5, pp. 1828-1837, Sept./Oct. 1980.

[3] V. Koritarov, L. Guzowski, J. Feltes, Y. Kazachkov, B. Lam, C. Grande-Moran, G. Thomann, L. Eng, B. Trouille, and P. Donalek, “Review of existing hydroelectric turbine,” Argonne National Laboratory, Lemont, IL, Tech. Rep. ANL/DIS-13/05, Aug. 2013.

[4] J. M. Merino and A. López, “ABB varspeed generator boosts efficiency and operating flexibility of hydropower plant,” *ABB Review*, vol. 3, pp. 33-38, 1996.

[5] A. Borghetti, M. Di Silvestro, G. Naldi, M. Paolone, and M. Alberti, “Maximum efficiency point tracking for adjustable-speed small hydro power plant,” presented at the 16th PSCC, Glasgow, Scotland, July 14-18, 2008.

[6] P. Lautier, C. O'Neil, H. J. N. Ndjana, C. Deschenes, R. Fraser, and M. Leclerc, “Variable-speed operation of a new very low head hydro turbine with low environmental impact,” in *Proc. 2007 IEEE Canada Electrical Power Conf.*, pp. 85-90.

[7] T. Kuwabara, A. Shibuya, H. Furuta, E. Kita, and K. Mitsuhashi, “Design and dynamic response characteristics of 400 MW adjustable speed pumped storage unit for Ohkawachi power station,” *IEEE Trans. Energy Convers.*, vol. 11, no. 2, June 1996.

[8] Available: http://en.wikipedia.org/wiki/Water_turbine#mediaviewer/File:Water_turbine_(en_2).svg

[9] V. Koritarov, L. Guzowski, J. Feltes, Y. Kazachkov, B. Gong, B. Trouille, and P. Donalek, “Modeling adjustable speed pumped storage hydro units employing doubly-fed induction machines,” Argonne National Laboratory, Lemont, IL, Tech. Rep. ANL/DIS-13/06, Aug. 2013.

[10] J. Janning and A. Schwery, “Next generation variable speed pump-storage power stations,” presented at EPE 2009, the 13th European Conference on Power Electronics and Applications, Barcelona, Spain, 2009.

[11] V. Koritarov, J. Feltes, Y. Kazachkov, B. Gong, P. Donalek, and V. Gevorgian, “Testing dynamic simulation models for different types of advanced pumped storage hydro units,” Argonne National Laboratory, Lemont, IL, Tech. Rep. ANL/DIS-13/08, Aug. 2013.